Article

Journal of
Nanoscience and Nanotechnology
Vol. 18, 132–142, 2018
www.aspbs.com/jnn

Role of Copper and Cerium on Core–Shell Al-MCM-41 in NO Reduction via a SCR-CH_4

Tanasan Intana[1], Karin Föttinger[2], Günther Rupprechter[2], and Paisan Kongkachuichay[1,*]

[1] *Department of Chemical Engineering, Faculty of Engineering, NANOTEC Center for Nanoscale Materials Design for Green Nanotechnology and Center for Advanced Studies in Nanotechnology and Its Applications in Chemical, Food and Agricultural Industries, Kasetsart University, Bangkok 10900, Thailand*
[2] *Institute of Materials Chemistry/Physical Chemistry Division, Vienna University of Technology, Getreidemarkt 9/1060, Vienna, Austria*

Copper species in the structure of Cu/core–shell Al-MCM-41 catalysts prepared by different techniques of Cu loading-substitution (S), ion-exchange (E), and impregnation (I) methods—were tested for NO reduction via a selective catalytic reaction with methane. Cerium was added to enhance the performance of copper. It was found that the 1.5%Ce-SEI-Cu/Al-MCM-41, in which Cu was loaded by all three techniques gave the highest NO conversion of 85% at 500 °C. Based on the results from FT-IR *in-situ* experiment, the mechanism of SCR-CH_4 reaction is proposed. The ion-exchange method gives the best performance of SCR-CH_4 reaction when compared with the other methods, because the Cu of reduced catalyst in this method exists in isolated Cu(I), which is an active site of the SCR-CH_4 reaction. With H_2O in the feed, the NO conversion of 1.5%-Ce-SEI-Cu/Al-MCM-41 catalyst is found to be rather stable.

Keywords: Cu, Ce, Al-MCM-41, NO, Reduction, SCR-CH_4.

1. INTRODUCTION

Transportation (mobile sources) and fuel combustion (stationary sources) are responsible for major amounts of pollutant emissions,[1] with released nitrogen oxides (NO_x) being particularly harmful to human health, not only by direct health risks but also by significant indirect effects, through their contribution of formation to the well-known smog and acid rain.[2–4] Selective catalytic reduction (SCR) is a good method to alleviate such problems by changing nitric oxide (NO), one of the NO_x, to nitrogen (N_2).[5–7] Seo et al.[8] have studied SCR with hydrocarbons for de-NO_x reaction and found that C_3H_8, from the alkane group gave better performance than C_3H_6, from the alkene group, as a reducing agent in the reaction. Methane (CH_4) has also been studied in much research[9–11] and has been used as a reducing agent in the SCR reaction, because it is the least reactive alkane. Based on the preceding considerations, selective catalytic reduction with methane (SCR-CH_4) with the use of catalysts was investigated in this work.

Catalysts have a significant role in the removal of NO via SCR-CH_4. There have been several metals—i.e., Cu,[12–14] Co,[15–17] Pd,[18–20] Pt,[21–23] Ag,[24–26] Ni,[27–29] Mn,[30–32] Fe,[33–35] In[36–38]—which were prepared by ion-exchange method with zeolites or impregnation method for use in SCR-CH_4 under the presence of excess oxygen. However, one problem is that the use of those catalysts was restricted by a narrow temperature range and low hydrothermal stability. Recently, many functional mesoporous materials have been studied.[39–43] Loading metal on Al-MCM-41 as a support can solve the problem of low hydrothermal stability when compared with zeolites support.[44] It was found that the use of Al-MCM-41 as the support also showed a high hydrothermal stability after heating to 800 °C in the presence of H_2O in SCR of NO with C_2H_4; the Al-MCM-41 support is consequently more stabilized than the ZSM-5 support. Based on our previous work,[45] core–shell-structured Al-MCM-41 enhances the performance of NO reduction, and copper can be easily reduced from Cu(II) to Cu(I), which is an active site for de-NO_x catalytic reaction. On the other hand, the problem of hydrothermal stability can also be improved by adding Ce as a promoter. Costilla et al.[46] found that the presence of Ce enhanced the activity for NO conversion and the selectivity to N_2 on Pd/H-MOR catalyst in SCR-CH_4 in the presence of H_2O. Therefore in this work, Cu metal was modified by loading

*Author to whom correspondence should be addressed.

 1533-4880/2018/18/132/011 doi:10.1166/jnn.2018.14583

on core–shell Al-MCM-41 as a catalyst, and Ce metal was added as a promoter.

In our recent work,[47] loading of copper metal on core–shell Al-MCM-41 by different techniques—ion-exchange method, impregnation method, and substitution method—were characterized and the existence of different copper species in the structure was identified. We found that the copper species in the substitution method was introduced into the silica-aluminosilicate framework and was presented in the tetrahedral-coordinated positions, the copper species in the ion-exchange method was isolated Cu(II), which was surrounded by OH groups, and the copper species in the impregnation method was in the form of CuO crystal as the major phase. Moreover, the different states of copper obtained from these three techniques have different effects on the acid sites of the catalyst, especially on the Brønsted acid sites, when it is reduced by H_2. Those resulting behaviors are expected to differ when the catalysts are used in NO reduction. Therefore, the purpose of this work is to investigate the role of different copper species on the SCR-CH_4 under the presence and absence of H_2O in the feed. Cerium was chosen to be added into the Cu/Al-MCM-41 catalyst, and the influence of the presence of Ce, affecting the mechanism of SCR-CH_4 reaction, was also studied in order to understand the behavior of the reaction.

2. EXPERIMENTAL DETAILS

2.1. Preparation of Catalysts

Following our previous work,[48] a core–shell-structured Al-MCM-41—used as a catalytic support—was prepared by using sol–gel method with the molar ratio of 1 SiO_2:0.2 CTAB:100 H_2O (based on Al-MCM-41 gel composition), for which the Al_2O_3/SiO_2 molar ratio was fixed at 0.1. Briefly, the support was prepared by adding tetraethyl orthosilicate (TEOS: 98%, Sigma-Aldrich) into the mixed solution of aluminum nitrate ($Al(NO_3)_3 \cdot 9H_2O$: 98%, QREC) and cetyl trimethyl ammonium bromide (CTAB: 98%, APS Ajax Finechem), while it was being stirred at 40 °C. After stirring for 1 h, the pH value of the mixture was immediately adjusted to 6.5, and the mixture was stirred for another 5 h. The obtained mixture was then transferred to a Teflon-lined autoclave for hydrothermal treatment at 100 °C for 24 h. Next, the solid product was filtered, washed with distilled water, dried at 80 °C overnight, and calcined in air at 600 °C for 5 h.

Following Intana et al.,[47] copper loading was conducted by three methods: substitution (Su), ion exchange (Ex), and impregnation (Im). For the substitution method, copper nitrate solution ($Cu(NO_3)_2 \cdot 2.5H_2O$: 99.5%, LOBA Chemie) of a concentration of 1 wt% was mixed with $Al(NO_3)_3$ solution and slowly added into the CTAB solution during the gel preparation, as mentioned earlier. Then, the whole process was repeated again in the same way for producing the Al-MCM-41. The Cu^{2+} ion-exchanged Al-MCM-41 was prepared by stirring the Al-MCM-41 in 0.05 M copper nitrate solution at 80 °C for 12 h. Then, the solid material was filtered and washed thoroughly with DI water, and dried at 110 °C for 12 h. Finally, it was calcined at 400 °C for 2 h. For the impregnation method, 1 g of Al-MCM-41 was impregnated with 3.15 ml of $Cu(NO_3)_2 \cdot 2.5H_2O$ solution, preparing copper contents of 1.5 wt% and 10 wt%, and then it was dried at 110 °C and calcined in air at 400 °C for 2 h. In an additional method, the three previously mentioned methods were combined in one catalyst by successive preparation proceeding through the substitution (S), ion-exchange (E), and impregnation (I) methods (in that order). The resulting product is called SEI-Cu/Al-MCM-41 catalyst. Following this, an aqueous solution of ammonium cerium nitrate ($Ce(NO_3)_6(NH_4)_2$: 99%, Sigma-Aldrich) at a concentration of 1.5 wt% was added to a beaker containing SEI-Cu/Al-MCM-41 catalyst by using impregnation method. The catalyst was dried at 110 °C and calcined in air at 500 °C for 2 h.

2.2. Catalyst Characterization

The reducibility of copper and cerium on the catalysts were characterized with temperature-programmed reduction (TPR). Firstly, the catalyst was packed in an Inconel tube reactor (Inconel-600, O.D. 3/8 in), and then a continuous flow of H_2 and Ar (9.6% H_2 balanced with Ar) was passed through at 15 ml/min. Following this, the catalyst was heated from room temperature to 900 °C at a heating rate 5 °C/min. Then, H_2 consumption was monitored by using a Shimadzu gas chromatograph (GC-2014) equipped with a thermal conductivity detector (TCD).

The acidity of catalysts before and after reduction was determined by temperature-programmed desorption of ammonia (NH_3-TPD) analysis. A sample (0.1 g) was packed in a tubular reactor. Before the analysis, the air inside the reactor was removed, and then the reactor was heated isothermally at 400 °C for 1 h. After that, it was cooled down to 100 °C, and NH_3 (100 mbar) was injected into the reactor until the sample was saturated with NH_3. Subsequently, the adsorbed NH_3 was desorbed by heating the reactor from 100 to 700 °C at a rate of 5 °C/min. The amount of desorbed NH_3 gas was measured by a mass spectrometer (Balzers Prisma 260).

2.3. *In-Situ* FT-IR Spectroscopy for NO Adsorption

The Fourier transform infrared spectroscopy of NO adsorption was studied using a Bruker IFS 28 spectrometer equipped with a MCT detector at a resolution of 4 cm^{-1}. A sample was first added into the mold and pressed to get a circular tablet having a diameter of 1 cm by using a hydraulic press with the pressure of 3 MPa. Then, the pressed sample was put inside a FT-IR sample holder. In order to prepare a reduced sample, H_2 (100 mbar) and N_2 (400 mbar) were injected to the sample at 350 °C for 1 h. Subsequently, the gases were evacuated, and

the sample was cooled down to room temperature. Then, He (365.1 mbar), 10% NO balanced with He (1 mbar), CH_4 (1.2 mbar), and O_2 (2.1 mbar) were fed into the sample cell sequentially, and the FTIR spectra were measured by using treated catalyst as a background. After that, the sample was heated from room temperature up to 255 °C with a heating rate of 5 °C/min.

2.4. *In-Situ* FT-IR Spectroscopy for H_2O Adsorption

The sample was reduced following the steps as described in Section 2.3. After the gases were evacuated, the sample was cooled down to room temperature. Then, 10% NO balanced with He (1 mbar) and H_2O (1 mbar) were fed into the sample cell sequentially, and the FTIR spectra were measured by using treated catalyst as a background.

2.5. Catalyst Testing

The performances of various catalysts were tested in the SCR-CH_4. The reaction was carried out in a fixed bed reactor at atmospheric pressure. Before running the reaction, the catalyst was reduced by using H_2 at 350 °C for 2 h. The feed composition under dry conditions was 500 ppm NO, 1200 ppm CH_4, and 2% O_2 balanced with He, to give a total flow of 30 ml/min or 720 h^{-1} gas hourly space velocity (GHSV) (catalyst bed volume of 2.5 cm^3). Under wet conditions, in contrast, 3% H_2O was added to the feed specified above (and then balanced with He, as previously). The outlet gases were analyzed by using two gas chromatographs (GC-14A, Shimadzu)—one was equipped with an Unibeads C column at 30 °C (for detecting N_2 and O_2) and another one was equipped with a Porapak-Q column at 140 °C (for detecting NO, NO_2, CH_4, CO_2 and H_2O)—subsequently, NO conversion (X_{NO}) was calculated from following equation:

$$X_{NO}(\%) = \frac{[NO]_{inlet} - [NO]_{outlet}}{[NO]_{inlet}} \times 100 \qquad (1)$$

The selectivity of gaseous products were calculated from their detected amounts divided by an amount of NO consumed.

3. RESULTS AND DISCUSSION

3.1. Characterization of Catalysts

The reducibility of catalysts and the forms of copper species present were evaluated by H_2-TPR method. When the catalyst was prepared by three techniques of Cu loading in one catalyst, it can be seen that there are four peaks of reduction of Cu in the SEI-Cu/MCM-41 (see Fig. 1(a)). The peaks at 240 and 265 °C refer to one-step reduction of CuO to Cu.[49] The peak at 240 °C corresponds to the CuO cluster existing on the outside of the pore structure because it was easily reduced at low temperature. On the other hand, the peak at 265 °C can be attributed to the CuO cluster existing on the inside of the pore structure. Meanwhile, the peaks at 330 and 586 °C refer to the reduction of isolated Cu(II) to Cu(I) and reduction of isolated Cu(I) to Cu(0), respectively.[50,51] For the 10%-Im-Ce/Al-MCM-41, the four peaks at 510, 640, 700, and 815 °C refer to the reduction of Ce^{4+} to Ce^{3+}, Ce^{3+} to Ce^{2+}, Ce^{2+} to Ce^{+} and Ce^{+} to Ce^{0}, respectively (see Fig. 1(c)). This stepwise reduction of CeO_2 was also confirmed by the thermogravimetric analysis (TA instrument SDT 2960). Therefore, the broad peak and narrow peak at 580 °C for 1.5%-Ce-SEI-Cu/Al-MCM-41 (see Fig. 1(b)) could be a result of the reduction of Ce^{4+} to Ce^{2+} and reduction of isolated Cu(I) to Cu(0), respectively. This result confirms the existence of CeO_2 clusters in the 1.5%-Ce-SEI-Cu/Al-MCM-41 catalyst.

NH_3-TPD profiles of the catalysts before and after reduction and of the Al-MCM-41 support are shown in Figure 2. When the SEI-Cu/Al-MCM-41 was reduced, the amount of Brønsted acid sites, reflected in the area of the desorption peak at 200 °C, was seen to decrease because of the steaming effect from the reduction of CuO sites.[47] Then, the catalyst was modified by adding Ce. When the 1.5%-Ce-SEI-Cu/Al-MCM-41 was reduced at 350 °C, Ce^{4+} was reduced to Ce^{3+}, an important site for the prevention of the steaming effect after reduction, since Ce^{3+} can react with OH groups[46] from the small amount of water that results during the reduction of CuO phase. Due to the benefit of Ce^{3+}, the amount of Brønsted acid sites on the 1.5%-Ce-SEI-Cu/Al-MCM-41 is still the same as that on the pre-reduced 1.5%-Ce-SEI-Cu/Al-MCM-41 catalyst. For this reason, it is advantageous to use Ce with Cu for the reaction that occurs under wet condition.

3.2. NO Adsorption

Figure 3 shows peaks of NO adsorption on the reduced catalyst (left) and the oxidized catalyst (right). For the reduced catalyst, before the measurement, the catalyst was reduced at 350 °C; hence, it was not completely reduced to Cu(0). Due to the fact that Cu^{+} still existed and it was further oxidized by NO in feed to be Cu^{2+}. The peak at 1600–1630 cm^{-1} corresponds to NO_2 adsorbed on Cu^{2+} (Cu^{2+}–NO_2), while that at 1810 cm^{-1} corresponds to NO adsorbed on Cu^{+} (Cu^{+}–NO). This means the Cu^{+} is the active site of catalyst in the SCR reaction.[44,52] Other peaks can also be ascribed as follows: the peak at 1900–1910 cm^{-1} corresponds to NO adsorbed on Cu^{2+} (Cu^{2+}–NO), the peak at 2250 cm^{-1} corresponds to N_2O adsorption, and the peak at 2150 cm^{-1} corresponds to NO^{+} adsorbed on Brønsted acid sites of the catalyst ($NO^{+}Z^{-}$) acting like an intermediate in the mechanism of SCR-CH_4.[38] For the oxidized catalyst, the catalyst exhibits higher adsorption capacity of NO and NO_2 on Cu^{2+} than the reduced catalyst, due to the larger amount of Cu^{2+} formed by oxidation.

When the gases were removed under vacuum condition, for the reduced catalyst it was found that the peak at 1810 cm^{-1} disappeared, demonstrating the weak

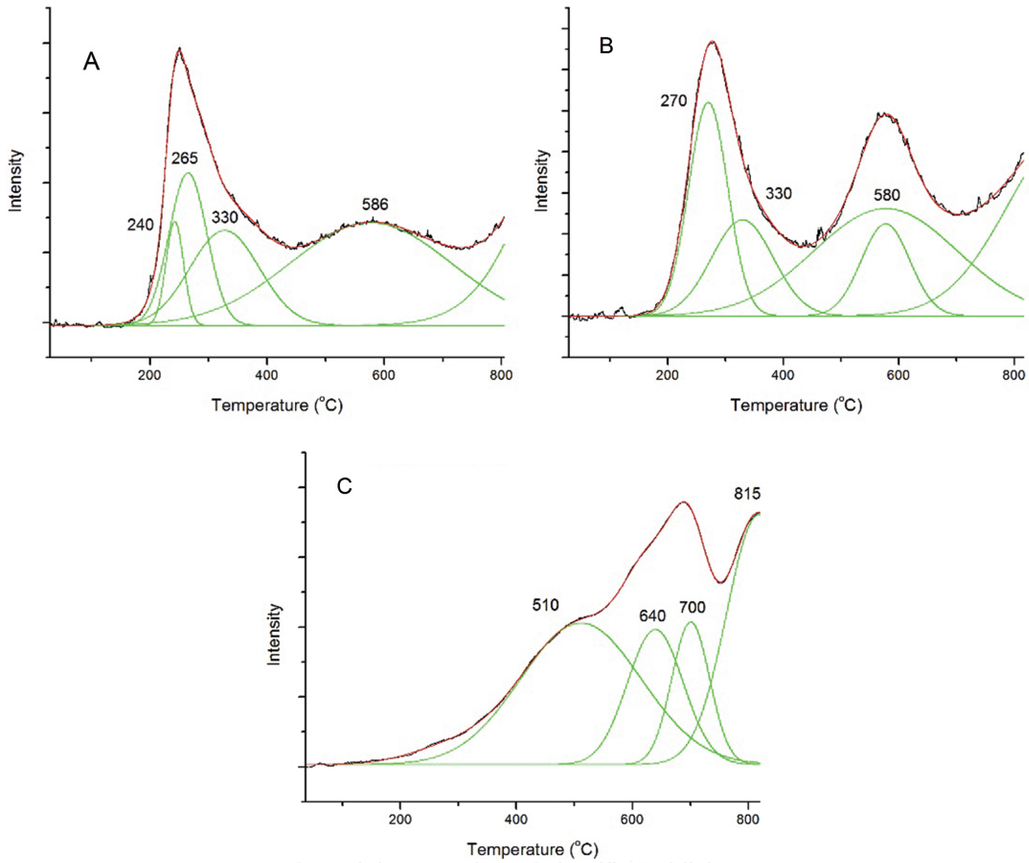

Figure 1. H_2 TPR profiles for Cu/core–shell Al-MCM-41 with different methods of preparation. (A) SEI-Cu/Al-MCM-41, (B) 1.5%-Ce-SEI-Cu/Al-MCM-41 and (C) 10%-Im-Ce/Al-MCM-41. Dashed line represents the fitting results.

adsorption of NO adsorbed on Cu^+—a good property for active sites. For both catalysts, the peak at 1910 cm^{-1} (i.e., Cu^{2+}–NO) decreased about 50% (almost disappeared in case of the reduced catalyst); this means that there

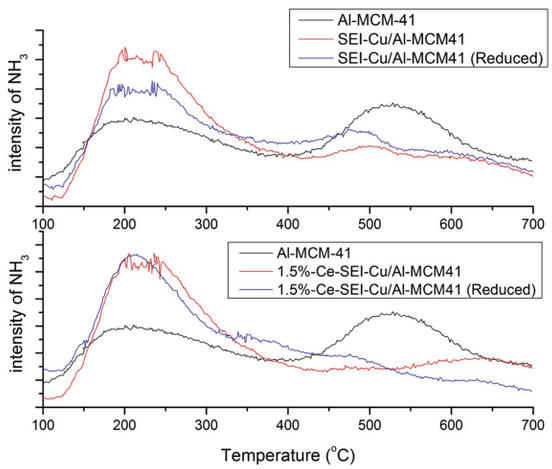

Figure 2. NH_3-TPD profiles of SEI-Cu/Al-MCM-41 and 1.5%-Ce-SEI-Cu/Al-MCM-41 before and after reduction compare with core–shell Al-MCM-41 as only support.

was medium adsorption of NO on Cu^{2+}. The two remaining peaks (those at 1630 and 2150 cm^{-1}) still have the same height when compared to the NO adsorption line; this means that the interaction between NO^+ and Brønsted acid sites and NO_2 and Cu^{2+} can be classified as a strong adsorption.

3.3. Simulation of SCR-CH_4 in *In-Situ* FT-IR

3.3.1. For SEI-Cu/Al-MCM-41

After adding He and NO on the reduced catalyst (see Fig. 4), the peak of Cu^+–NO, which had appeared since 3 min after loading, gradually increased up to 14 min, thereby showing that there is a high amount of Cu^+ as the active sites of the catalyst. The peak corresponding to Cu^{2+}–NO appeared starting 5 minutes after loading, together with the peak at 2250 cm^{-1} and gradually increased up to 14 min. This behavior indicates that Cu^+ was oxidized to Cu^{2+} by NO and produced N_2O in this step, and then it also produced NO–Cu^{2+}–O^- that was able to react with NO to form NO–Cu^{2+}–NO_2^-, confirmed by a corresponding peak around 1600 cm^{-1}. These phenomena are in agreement with Cheung et al.[53] Additionally, the NO reacted with Brønsted acid sites to form NO^+Z^-

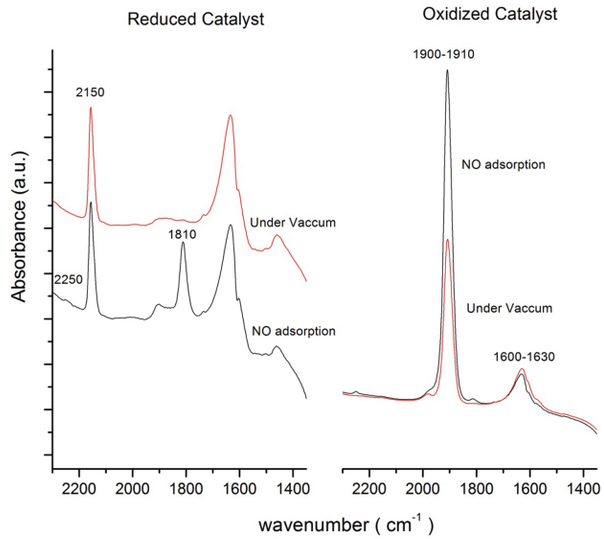

Figure 3. Spectra of FT-IR *in-situ* NO adsorption on Cu/Al-MCM-41: NO adsorption (black line) and removal of NO gas under vacuum (red line).

as identified at 2156 cm^{-1} by following reaction:[54]

$$NO + 2H^+ - OZ \longleftrightarrow NO^+ - OZ + HO - H^+ - Z \quad (2)$$

The results of adding CH_4 to the sample cell are shown in Figure 5. There are peaks around 3150–3000 cm^{-1} corresponding to the spectra of CH_4 in the system; these peaks appeared during an interval of 3 min to 7 min after starting measurement. Subsequently, O_2 was added (see Fig. 6); it can be seen that the peak of Cu(I) was dramatically decreased with respect to oxidation of Cu(I). On the other hand, the peak of Cu(II) clearly increased in height, due to an effect of oxidizing Cu(I) to Cu(II) by O_2. Moreover, the addition of O_2 facilitated the reaction between NO and O_2 on Brønsted acid sites in the catalyst[55] and produced NO_2 gas (seen at 1600–1630 cm^{-1}). Subsequently, the NO and

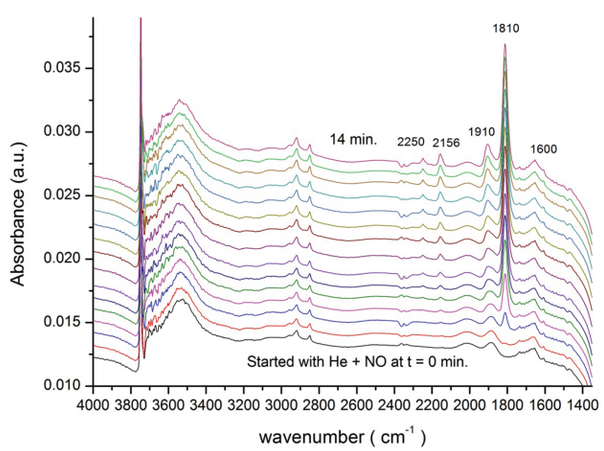

Figure 4. Spectra of FT-IR *in-situ* on reduced SEI-Cu/Al-MCM-41 after adding He + NO.

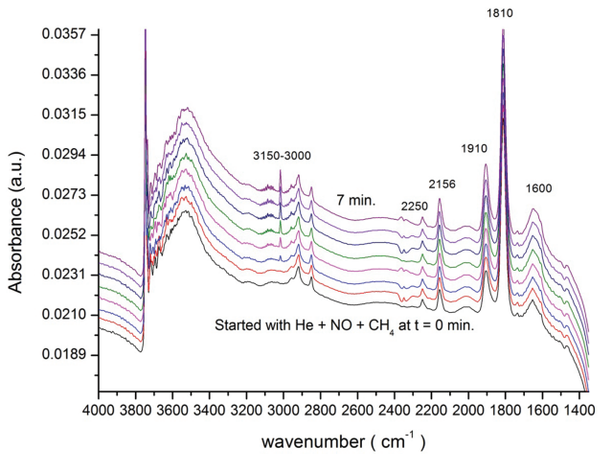

Figure 5. Spectra of FT-IR *in-situ* on reduced SEI-Cu/Al-MCM-41 after adding He + NO + CH_4.

NO_2 reacted on the Cu(0) or Brønsted acid sites, forming NO^+ adsorbed on the Brønsted acid sites (NO^+Z^-) as an intermediate and producing H_2O molecules, which can be seen as the corresponding peak at 3600 cm^{-1}, in accordance with Eq. (3).

$$NO + NO_2 + 2H^+Z^- \longleftrightarrow 2NO^+Z^- + H_2O \quad (3)$$

All of the preceding can be seen in the increasing width and height of the peak at 2156 cm^{-1}, such that it overlaps and eventually swallows up the smaller peak at 2250 cm^{-1}. This behavior is indicative of one of the steps to convert NO to N_2 in the proposed mechanism of SCR-CH_4 (cf. the later subsection discussing the mechanism).

3.3.2. For 1.5%-Ce-SEI-Cu/Al-MCM-41

For Cu/Al-MCM-41 catalyst promoted with Ce, the spectra of NO adsorption after reduction are shown in Figure 7.

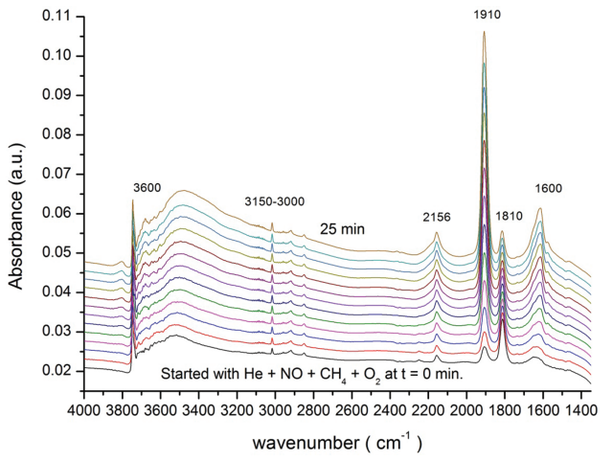

Figure 6. Spectra of FT-IR *in-situ* on reduced SEI-Cu/Al-MCM-41 after adding He + NO + CH_4 + O_2.

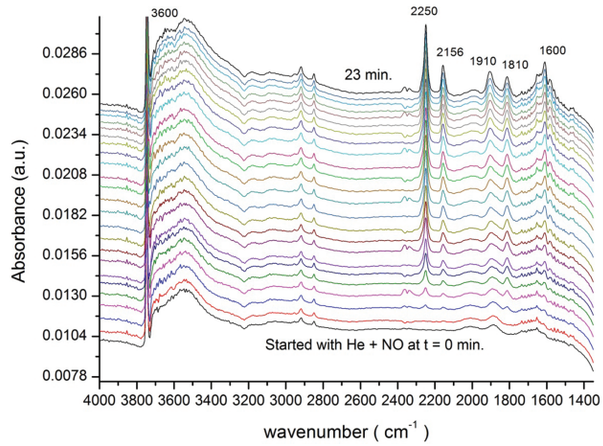

Figure 7. Spectra of FT-IR *in-situ* on reduced 1.5%-Ce-SEI-Cu/Al-MCM-41 after adding He + NO.

The influence of the Ce is observed by the increasing of the peak around 1600 cm^{-1}, meaning that the Ce catalyzes the NO to NO_2,[56] and then both of them (NO and NO_2) are able to oxidize Cu^+ to Cu^{2+} and produce N_2O. This explanation is supported by increasing of the peak at 1910 cm^{-1}, overtaking the value of the peak at 1810 cm^{-1}, and becoming the highest peak at 2250 cm^{-1}. Additionally, the NO and NO_2 are able to react on Brønsted acid sites to form NO^+Z^- (seen at 2156 cm^{-1}) and produce H_2O molecules, causing an occurrence of the peak at 3600 cm^{-1}.

When CH_4 was added into the system (see Fig. 8), Ce metal facilitated the change of NO to NO_2, and CH_4 was protonated to form a transient CH_5^+ on the Brønsted acid sites. Subsequently, the CH_5^+ reacted with NO_2 to form CH_3NO^+ and H_2O;[57] as a result, the peaks around 3016–3625 cm^{-1} increased in intensity. After that, the CH_3NO^+ reacted on Cu^+ sites to form NO^+Z^- and oxidized Cu^+ to Cu^{2+}. In the form of chemical equations, one then has the following reactions:

$$CH_4 + H^+ - Z^- \longrightarrow CH_5^+ - Z^- \xrightarrow{NO_2} CH_3NO^+ - Z^- + H_2O \quad (4)$$

$$Cu^+ - OH + CH_3NO^+ - Z^- \longrightarrow NO^+Z^- + Cu^{2+} - O + CH_4 \quad (5)$$

It can be concluded that CH_4 in the system has an effect on NO_2 in creating the intermediate sites (i.e., NO^+Z^-). This explanation is supported by the increase in both peaks at 1910 cm^{-1} and 2156 cm^{-1}.

After CH_4 and O_2 were added in the system, the obtained spectra of FT-IR are shown in Figure 9. The behaviors of this system are like those of SEI-Cu/Al-MCM-41 catalyst without Ce, but the intensity of the peaks at 3600, 2156, and 1630 cm^{-1} are higher than those for the catalyst without Ce. The fact that both Ce and O_2 catalyze the NO to NO_2 and create a considerable amount of intermediate sites supports the notion that one could attain better performance of SCR-CH_4.

3.3.3. Mechanism of SCR-CH_4 Reaction

After adding all of the reactant gases (i.e., NO, CH_4, O_2, and He) into the sample cell, the SEI-Cu/Al-MCM-41 catalyst was heated from room temperature to 255 °C (see Fig. 10). The peak at 3500 cm^{-1}, corresponding to copper surrounded by OH groups on the surface of catalyst, was decreased in height with increasing temperature. Such behavior indicates the loss of water in the structure of the catalyst, by as per Eq. (6). The two peaks between 3000 and 2850 cm^{-1}, corresponding to stretching of C–H molecules, also decreased in size, meaning that there occurred decomposition of CH_4 in the system. When the temperature was raised above 150 °C, there were no NO molecules adsorbed on the catalyst. This might indicate that the NO started changing to N_2, because the rate of adsorption and desorption of molecules on the catalyst

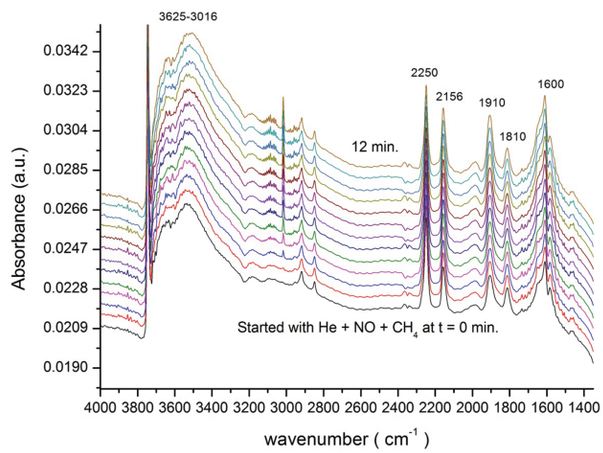

Figure 8. Spectra of FT-IR *in-situ* on reduced 1.5%-Ce-SEI-Cu/Al-MCM-41 after adding He + NO + CH_4.

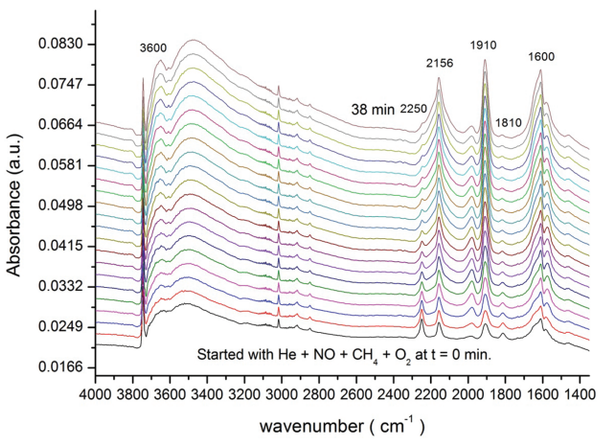

Figure 9. Spectra of FT-IR *in-situ* on reduced 1.5%-Ce-SEI-Cu/Al-MCM-41 after adding He + NO + CH_4 + O_2.

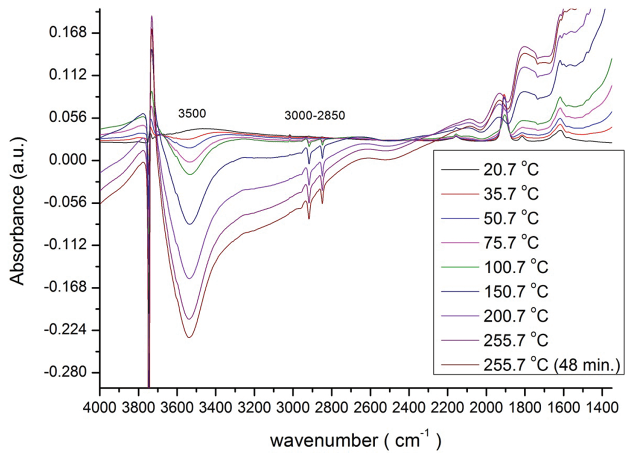

Figure 10. Spectra of FT-IR *in-situ* on reduced SEI-Cu/Al-MCM-41 in SCR-CH_4 reaction at different temperature.

was very fast at high temperature. Based on the obtained *in-situ* FT-IR results, the mechanism of SCR-CH_4 reaction using SEI-Cu/Al-MCM-41 as a catalyst is proposed as follows:

$$Cu^+OH^- + H^+ - Z^- \xrightarrow{\text{Heat}} Cu^+ - Z^- + H_2O \quad (6)$$

$$Cu^+ - Z^- + NO \text{ or } NO_2 \longrightarrow NO - Cu^+ - Z^- \text{ or } NO_2 - Cu^+ - Z^- \quad (7)$$

$$NO - Cu^+ - Z^- + O_2 + NO \longrightarrow Cu^+NO_3^- + NO^+ - Z^- \quad (8)$$

$$NO_2 - Cu^+ - Z^- + NO_2 \longrightarrow Cu^+NO_3^- + NO^+ - Z^- \quad (9)$$

$$Cu^+NO_3^- + CH_4 \longrightarrow CH_3NO_2 + Cu^+OH^- \quad (10)$$

$$CH_3NO_2 + NO^+ - Z^- \longrightarrow N_2 + CO_2 + H_2O + H^+ - Z^- \quad (11)$$

Note that, for 1.5%-Ce-SEI-Cu/Al-MCM-41, the spectra (not shown) of running the reaction were like those in Figure 10 as well.

The results of FT-IR spectra are presented in Figure 11 for SEI-Cu/Al-MCM-41 and 1.5%-Ce-SEI-Cu/Al-MCM-41 catalysts. When the NO was added to the system, the peak of Cu(I) on 1.5%-Ce-SEI-Cu/Al-MCM-41 is found to be lower than that for SEI-Cu/Al-MCM-41 catalyst, because Cu(II) species were covered by CeO_4 and were hard to be reduced to Cu(I). However, when O_2 was added to the system, the peak at 2150 cm^{-1} was, for 1.5%-Ce-SEI-Cu/Al-MCM-41, higher than the peak for SEI-Cu/Al-MCM-41 at the same wavenumber. Based on these FT-IR results, it would be reasonable to predict that creating a considerable amount of intermediate sites in the reaction can facilitate the performance of the catalyst, and the performance of 1.5%-Ce-SEI-Cu/Al-MCM-41 would be better than that of the SEI-Cu/Al-MCM-41 catalyst.

3.3.4. Effect of H_2O on Catalysts

When the catalyst was reduced at 350 °C by H_2 and then cooled down to room temperature, the catalyst was adsorbed by NO gas (shown as the NO adsorption line in Fig. 12). There are two peaks, one at 1809 cm^{-1} and another one at 1,909 cm^{-1}, corresponding to Cu^+–NO and

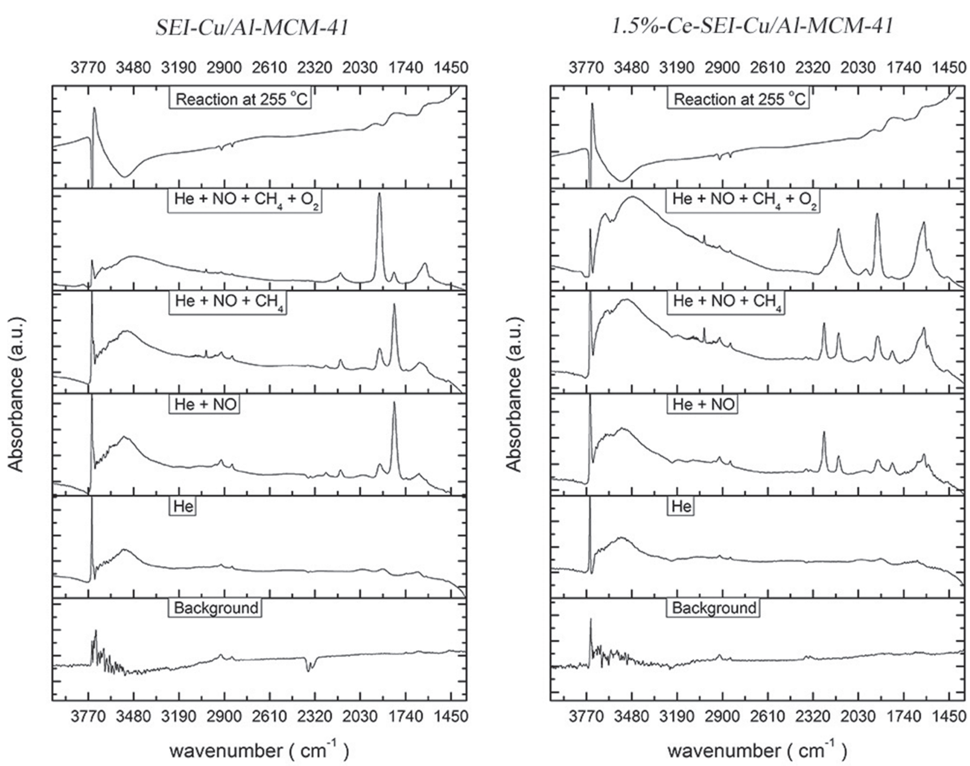

Figure 11. Summary of FT-IR *in-situ* spectra in SCR-CH_4 on SEI-Cu/Al-MCM-41 (left) and 1.5%-Ce-SEI-Cu/Al-MCM-41 (right).

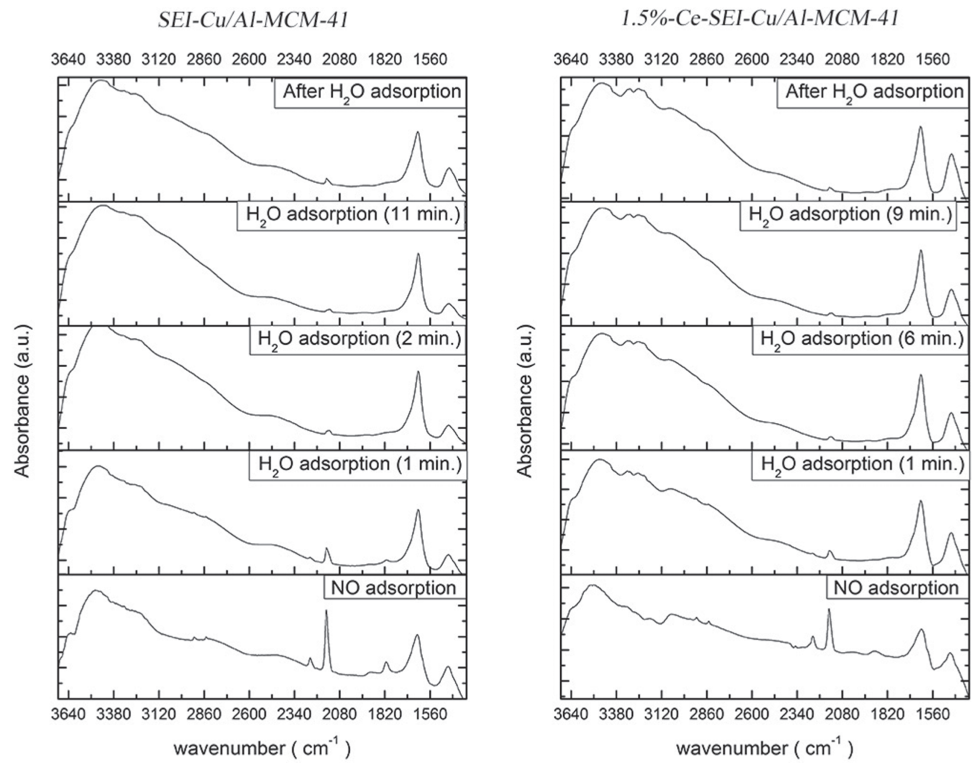

Figure 12. Spectra of *in-situ* FT-IR for H_2O adsorption on reduced SEI-Cu/Al-MCM-41 (left) and 1.5%-Ce-SEI-Cu/Al-MCM-41 (right).

Cu^{2+}–NO, respectively. After the addition of water in the system, the peak of Cu^{+}–NO was dramatically decreased for both catalysts. This indicates that the water has a negative effect on the active sites of the catalysts, making the catalytic performance of the catalyst decrease when being used under wet condition.

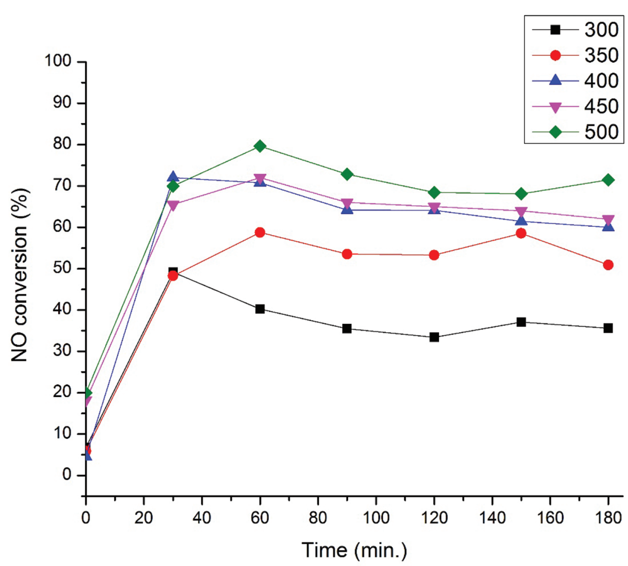

Figure 13. NO conversion of 1.5%-Im-Cu/Al-MCM-41 in SCR-CH_4 at different temperature (300–500 °C) for 3 h.

3.4. Catalytic Performance

The 1.5%-Im-Cu/Al-MCM-41 catalyst was tested via SCR-CH_4 reaction at different temperatures (300–500 °C) for 3 h (see Fig. 13). It was found that the NO conversion increased while the temperature was increased. The highest average NO conversion of 72% was obtained at 500 °C. Given this result, the temperature at 500 °C was used for testing the performance of the other catalysts.

Figure 14 shows the performances of all catalysts tested in SCR-CH_4 at 500 °C for 3 h. The substitution method (1%-Su-Cu/Al-MCM-41) gives the lowest NO conversion, having an average NO conversion of 58% because copper atoms exist in the tetrahedral-coordinated position and this structure is relatively stable.[47] The impregnation method at high copper loading (10%-Im-Cu/Al-MCM-41) gives low NO conversion at the beginning because the copper species were full of Cu(0) due to reducing of CuO crystals, which constitute the main copper species in this method.[47] After 1 h, the NO conversion was increased to 73%. This observation can be explained as follows: Cu(0) might be partial oxidized to Cu(I) by O_2 in the system, becoming the active sites. At low copper loading (1.5%-Im-Cu/Al-MCM-41), the copper species were CuO crystals and isolated Cu(II).[47] When the 1.5%-Im-Cu/Al-MCM-41 catalyst was reduced by H_2, the isolated Cu(II) was changed to Cu(I). Therefore, the Cu(I) from reducing of isolated Cu(II) was active at the beginning and gave an average NO conversion of

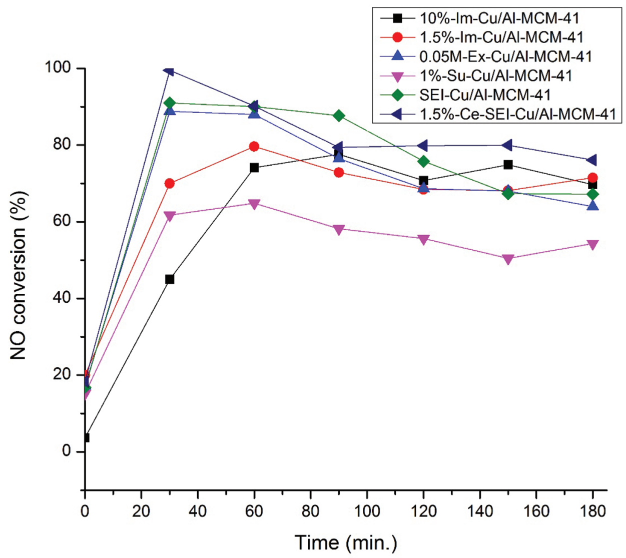

Figure 14. NO conversion of different catalysts in SCR-CH_4 at 500 °C for 3 h.

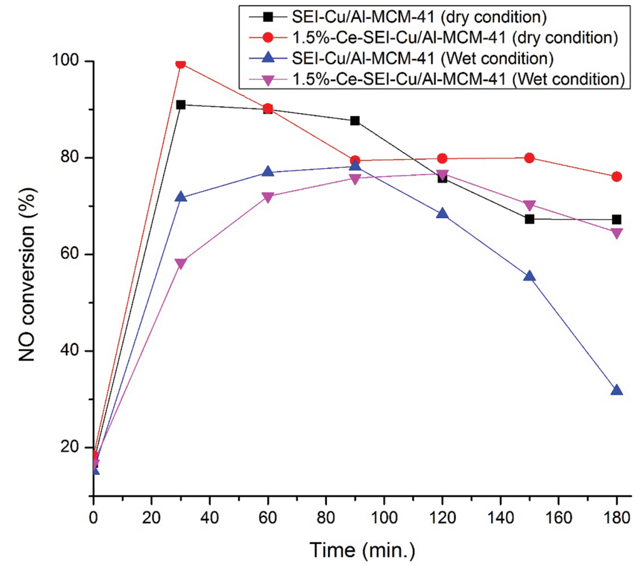

Figure 16. NO conversion on SEI-Cu/Al-MCM-41 and 1.5%-Ce-SEI-Cu/Al-MCM-41 in presence and absence of water for SCR-CH_4 at 500 °C for 3 h.

71%. The ion-exchange method (0.05M-Ex-Cu/Al-MCM-41) gave the highest NO conversion (about 78%) when compared to the substitution and impregnation methods. The copper atoms in the ion-exchange method exist in the isolated Cu(II)[47] and they were reduced to Cu(I), which is the active site of the SCR-CH_4 reaction. Consequently, it can be concluded that the Cu(I) sites play the essential role in this reaction.[58] When the catalyst was prepared by combined three methods: substitution, ion-exchange, and impregnation (SEI-Cu/Al-MCM-41), the average NO conversion was increased up to 80%. Interestingly, when Ce was loaded on the SEI-Cu/Al-MCM-41 catalyst (1.5%-Ce-SEI-Cu/Al-MCM-41), the highest average NO conversion of 85% was achieved, because Ce promotes creation of intermediate sites in the reaction. It can be supposed that the intermediate sites encourage the catalytic performance of SCR-CH_4 reaction, as confirmed by FT-IR results.

Based on the obtained chromatographs from the GCs, peak that corresponds to N_2O was not observed. Therefore, selectivity of only N_2 and NO_2 are presented in Figure 15. The results indicate that when there is high amount of NO_2 in the system, the production of N_2 will be facilitated by the Ce sites on the catalyst. This reason emphasizes the role of Ce as described in Section 3.3.3. It should be noted that the N_2 selectivity obtained from both catalysts: SEI-Cu/Al-MCM-41 and 1.5%-Ce-SEI-Cu/Al-MCM-41 is about 3.2 times of the NO_2 selectivity. It means that N_2 is the main product of the SCR-CH_4 when these catalysts were used.

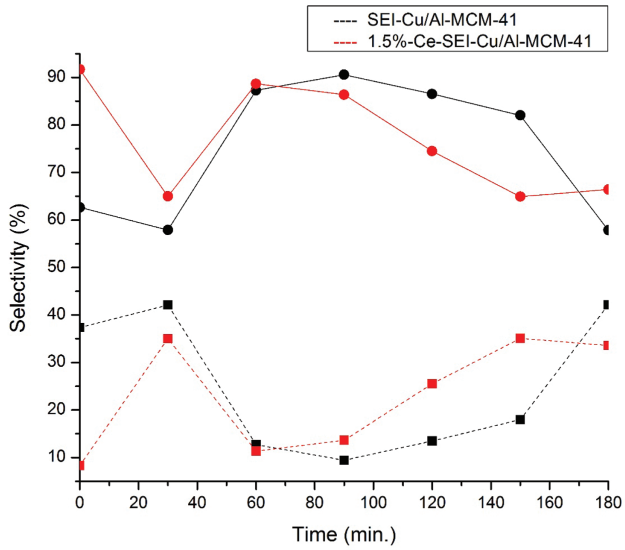

Figure 15. Selectivity of N_2 (–●–) and NO_2 (– –■– –) for SEI-Cu/Al-MCM-41 (black line) and 1.5%-Ce-SEI-Cu/Al-MCM-41 (red line).

Finally, the SEI-Cu/Al-MCM-41 and 1.5%-Ce-SEI-Cu/Al-MCM-41 catalysts were tested for the SCR-CH_4 at 500 °C for 3 h with 3% water added in the feed (see Fig. 16). It is found that the catalytic performance of both catalysts was decreased when compared to the dry condition. In particular, for the SEI-Cu/Al-MCM-41 catalyst, it can be seen that the NO conversion lessens after 90 min. However, for the 1.5%-Ce-SEI-Cu/Al-MCM-41 catalyst, the NO conversion is rather stable, proving that the Ce^{3+} was able to protect against the water in the feed reacting with the active sites and made the stability last longer under the wet condition.

4. CONCLUSIONS

The different copper species prepared by substitution, ion-exchange, and impregnation methods were investigated for using in SCR-CH_4 reaction. The

ion-exchange method (0.05M-Ex-Cu/Al-MCM-41) having isolated Cu(II) species gave the highest NO conversion when compared to the results from the substitution and impregnation methods. The reduced catalyst from this method gave isolated Cu(I), which is the active site of SCR-CH_4 reaction. In addition, the catalyst prepared by the combination of substitution, ion-exchange, and impregnation methods yielded the NO conversion of 80%.

The study of SCR-CH_4 reaction via FT-IR spectra shows that the role of Ce is in catalyzing NO to NO_2, and the NO_2 can react to NO or CH_4 on Brønsted acid sites, creating a considerable amount of NO^+Z^-, which acts as intermediate sites in the proposed reaction mechanism of SCR-CH_4. This promotes the catalytic performance of SCR-CH_4 reaction, as confirmed by testing the reaction on 1.5%-Ce-SEI-Cu/Al-MCM-41 catalyst, which was found to give the highest NO conversion (85%). Under wet condition, the NO conversion of 1.5%-Ce-SEI-Cu/Al-MCM-41 catalyst is rather stable, indicating that the other role of Ce on the catalyst lies in the reaction of Ce^{3+} with OH groups and the protection against small amounts of water reacting with the active sites, thus making the stability of the catalyst longer-lasting.

Acknowledgments: This work was supported by the Thailand Research Fund (TRF) through the Royal Golden Jubilee Ph.D. Program (Grant No. PHD/0051/2553 for T. Intana) and the Kasetsart University Research and Development Institute (KURDI).

References and Notes

1. M. Chen and J. W. Chu, *J. Clean. Prod.* 19, 1266 (**2011**).
2. I. M. R. Fattah, M. H. Hassan, M. A. Kalam, A. E. Atabani, and M. J. Abedin, *J. Clean. Prod.* 79, 82 (**2014**).
3. J. V. Caneghem, J. D. Greef, C. Block, and C. Vandecasteele, *J. Clean. Prod.* 112, 4452 (**2016**).
4. Z. B. Xiong, Q. Hu, D. Y. Liu, C. Wu, F. Zhou, Y. Z. Wang, J. Jin, and C. M. Lu, *Fuel* 165, 432 (**2016**).
5. J. Baleta, M. Vujanović, K. Pachler, and N. Duić, *J. Clean. Prod.* 88, 280 (**2015**).
6. P. Wang, H. Sun, X. Quan, and S. Chen, *J. Hazard. Mater.* 301, 512 (**2016**).
7. X. Zhao, L. Huang, H. Li, H. Hu, X. Hu, L. Shi, and D. Zhang, *Appl. Catal. B: Environ.* 183, 269 (**2016**).
8. C. K. Seo, B. Choi, H. Kim, C. H. Lee, and C. B. Lee, *Chem. Eng. J.* 191, 331 (**2012**).
9. J. C. Martín, S. B. Rasmussen, S. Suárez, M. Yates, F. J. Gil-Llambías, M. Villarroel, and P. Ávila, *Appl. Catal. B: Environ.* 91, 423 (**2009**).
10. M. Foix, C. Guyon, M. Tatoulian, and P. D. Costa, *Catal. Commun.* 12, 20 (**2010**).
11. L. Gutierrez, A. Boix, H. Decolatti, H. Solt, F. Lónyi, and E. Miró, *Microporous Mesoporous Mater.* 163, 307 (**2012**).
12. Z. Schay, L. Guczi, A. Beck, I. Nagy, V. Samuel, S. P. Mirajkar, A. V. Ramaswamy, and G. P. Borbély, *Catal. Today* 75, 393 (**2002**).
13. Y. Li, J. Su, J. Ma, F. Yu, J. Chen, and R. Li, *Catal. Commun.* 65, 6 (**2015**).
14. B. Ivanov, I. Spassova, M. Milanova, G. Tyuliev, and M. Khristova, *J. Rare Earth* 33, 382 (**2015**).
15. P. J. Smeets, Q. Meng, S. Corthals, H. Leeman, and R. A. Schoonheydt, *Appl. Catal. B: Environ.* 84, 505 (**2008**).
16. S. Chen, X. Yan, Y. Wang, J. Chen, D. Pan, J. Ma, and R. Li, *Catal. Today* 175, 12 (**2011**).
17. F. Lónyi, H. E. Solt, Z. Pászti, and J. Valyon, *Appl. Catal. B: Environ.* 150, 218 (**2014**).
18. A. P. Ferreira, S. Capela, P. D. Costa, C. Henriques, M. F. Ribeiro, and F. R. Ribeiro, *Catal. Today* 119, 156 (**2007**).
19. S. Capela, R. Catalão, M. F. Ribeiro, P. D. Costa, G. D. Mariadassou, F. R. Ribeiro, and C. Henriques, *Catal. Today* 137, 157 (**2008**).
20. H. Decolatti, H. Solt, F. Lónyi, J. Valyon, E. Miró, and L. Gutierrez, *Catal. Today* 172, 124 (**2011**).
21. F. Lónyi, J. Valyon, L. Gutierrez, M. A. Ulla, and E. A. Lombardo, *Appl. Catal. B: Environ.* 73, 1 (**2007**).
22. S. S. Kim, S. H. Choi, S. M. Lee, and S. C. Hong, *J. Ind. Eng. Chem.* 18, 272 (**2012**).
23. R. P. Hernández, A. G. Cortés, J. A. Alatorre, S. Rojas, R. Mariscal, J. L. G. Fierro, and G. Díaz, *Catal. Today* 107, 149 (**2005**).
24. X. She, M. F. Stephanopoulos, C. Wang, Y. Wang, and C. H. F. Peden, *Appl. Catal. B: Environ.* 88, 98 (**2009**).
25. K. N. Rao and H. P. Ha, *Appl. Catal. A: Gen.* 433, 162 (**2012**).
26. F. Gunnarsson, M. Z. Granlund, M. Englund, J. Dawody, L. J. Pettersson, and H. Härelind, *Appl. Catal. B: Environ.* 162, 583 (**2015**).
27. M. Mihaylov, K. Hadjiivanov, and D. Panayotov, *Appl. Catal. B: Environ.* 51, 33 (**2004**).
28. D. Pietrogiacomi, M. C. Campa, and M. Occhiuzzi, *Catal. Today* 227, 116 (**2014**).
29. M. C. Campa, D. Pietrogiacomi, and M. Occhiuzzi, *Appl. Catal. B: Environ.* 168, 293 (**2015**).
30. A. W. Aylor, L. J. Lobree, J. A. Reimer, and A. T. Bell, *J. Catal.* 170, 390 (**1997**).
31. M. C. Campa, D. Pietrogiacomi, S. Tuti, G. Ferraris, and V. Indovina, *Appl. Catal. B: Environ.* 18, 151 (**1998**).
32. N. Li, A. Wang, X. Wang, M. Zheng, R. Cheng, and T. Zhang, *Appl. Catal. B: Environ.* 48, 259 (**2004**).
33. A. V. Boix, J. M. Zamaro, E. A. Lombardo, and E. E. Miró, *Appl. Catal. B: Environ.* 46, 121 (**2003**).
34. Q. Shen, L. Li, C. He, H. Tian, Z. Hao, and Z. P. Xu, *Appl. Catal. B: Environ.* 91, 262 (**2009**).
35. J. Janas and S. Dzwigaj, *Catal. Today* 176, 272 (**2011**).
36. B. Gil, J. Janas, E. Wloch, Z. Olejniczak, J. Datka, and B. Sulikowski, *Catal. Today* 137, 174 (**2008**).
37. F. Lónyi, H. E. Solt, J. Valyon, H. Decolatti, L. B. Gutierrez, and E. Miró, *Appl. Catal. B: Environ.* 100, 133 (**2010**).
38. F. Lónyi, H. E. Solt, J. Valyon, A. Boix, and L. B. Gutierrez, *Appl. Catal. B: Environ.* 117, 212 (**2012**).
39. Z. Huang and S. Che, *Bull. Chem. Soc. Jpn* 88, 617 (**2015**).
40. E. Yamamoto and K. Kuroda, *Bull. Chem. Soc. Jpn.* 89, 501 (**2016**).
41. V. Malgras, Q. Ji, Y. Kamachi, T. Mori, F. K. Shieh, K. C. W. Wu, K. Ariga, and Y. Yamauchi, *Bull. Chem. Soc. Jpn* 88, 1171 (**2015**).
42. W. R. Erwin, H. F. Zarick, E. M. Talbert, and R. Bardhan, *Energy Environ. Sci.* 9, 1577 (**2016**).
43. Y. Chen and J. Shi, *Adv. Mater.* 28, 3235 (**2016**).
44. R. Q. Long and R. T. Yang, *Ind. Eng. Chem. Res.* 38, 873 (**1999**).
45. B. Chamnankid, S. Rattanaporn, and P. Kongkachuichay, *J. Nanosci. Nanotechnol.* 12, 9325 (**2012**).
46. I. O. Costilla, M. D. Sanchez, M. A. Volpe, and C. E. Gigola, *Catal. Today* 172, 84 (**2011**).
47. T. Intana, K. Föttinger, G. Rupprechter, and P. Kongkachuichay, *Colloids Surf. A* 467, 157 (**2015**).
48. B. Chamnankid, T. Witoon, P. Kongkachuichay, and M. Chareonpanich, *Colloids Surf. A* 380, 319 (**2011**).
49. S. Kiatphuengporn, M. Chareonpanich, and J. Limtrakul, *Chem. Eng. J.* 240, 527 (**2014**).
50. L. Kundakovic and M. Flytzani-Stephanopoulos, *Appl. Catal. A: Gen.* 171, 13 (**1998**).

51. M. S. Batista, R. A. A. Melo, M. Wallau, and E. A. Urquieta-Gonzalez, *Brazilian J. Chem. Eng.* 22, 433 **(2005)**.
52. J. Dědeček, L. Čapek, P. Sazama, Z. Sobalík, and B. Wichterlová, *Appl. Catal. A: Gen.* 391, 244 **(2011)**.
53. T. Cheung, S. K. Bhargava, M. Hobday, and K. Foger, *J. Catal.* 158, 301 **(1996)**.
54. S. A. Skarlis, D. Berthout, A. Nicolle, and C. Dujardin, *Appl. Catal. B: Environ.* 148, 446 **(2014)**.
55. Y. Traa, B. Burger, and J. Weitkamp, *Microporous Mesoporous Meter.* 30, 3 **(1999)**.
56. J. A. Z. Pieterse and S. Booneveld, *Appl. Catal. B: Environ.* 73, 327 **(2007)**.
57. J. Y. Yan, H. H. Kung, W. M. H. Sachtler, and M. C. Kung, *J. Catal.* 175, 294 **(1998)**.
58. H. Yahiro and M. Iwamoto, *Appl. Catal. A: Gen.* 222, 163 **(2001)**.

Received: 30 November 2016. Accepted: 26 December 2016.